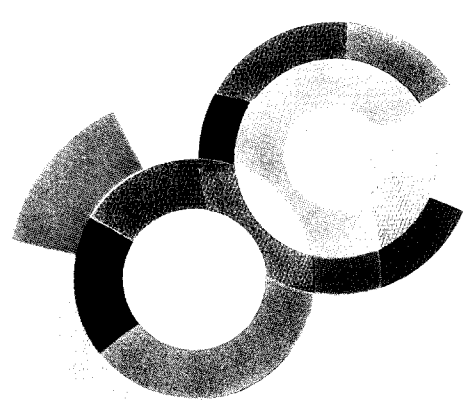
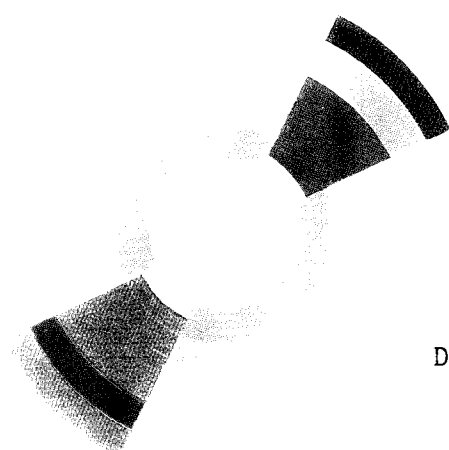
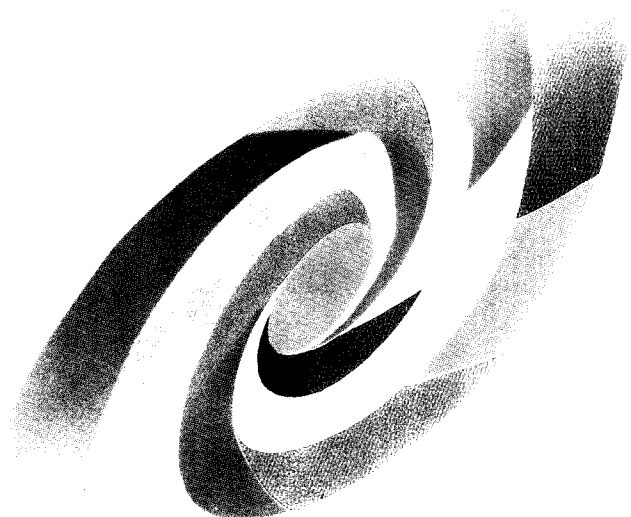


DAPNIA - SPHn 94-10
SC 9416



DAPNIA/SPHn 94 10

03/1994

DISSIPATIVE ASPECTS IN PROJECTILE
FRAGMENTATION AT 200 MeV/U

C. Donzaud, D. Bachelier, C.O. Bacri,
R. Bimbot, B. Borderie, J.L. Boyard,
F. Clapier, T. Hennino, M.F. Rivet,
P. Roussel, C. Stephan, L. Tassan-Got,
D. Bazin, C. Grunberg, D. Disdier,
B. Lott, C. Volant

DAPNIA

Le DAPNIA (Département d'Astrophysique, de physique des Particules, de physique Nucléaire et de l'Instrumentation Associée) regroupe les activités du Service d'Astrophysique (SAp), du Département de Physique des Particules Élémentaires (DPhPE) et du Département de Physique Nucléaire (DPhN).

Adresse : DAPNIA, Bâtiment 141
CEA Saclay
F - 91191 Gif-sur-Yvette Cedex

Exposé invité au :

XXXII International Winter Meeting on

Nuclear Physics

Bormio, Italie

du 24 au 28 janvier 1994

DISSIPATIVE ASPECTS IN PROJECTILE FRAGMENTATION AT 200 MEV/U

C. Donzaud, D. Bachelier†, C.O. Bacri, R. Bimbot, B. Borderie,
J.L. Boyard, F. Clapier, T. Hennino, M.F. Rivet, P. Roussel,

C. Stephan, L. Tassan-Got
IPN Orsay

D. Bazin, CEN Bordeaux

C. Grunberg, GANIL Caen

D. Disdier, B. Lott, CRN Strasbourg

C. Volant CEA Saclay

Peripheral collisions induced by light projectiles at relativistic energies have been studied at the Bevalac facility in the 1970's [1]. Two different frameworks were then used to describe the fragmentation process: the participant-spectator model and the intranuclear cascade one. Whereas the excitation energy is related to the surface-energy excess of the deformed projectile spectator after the abrasion stage in the first one, it originates from the hole energy which cascade nucleons left in the volume of the projectile remnant as well as from the energy of cascade nucleons trapped in the remnant in the second one. In spite of the different fragment yields predicted, these two models provide approximatively the same final isotopic distributions after the evaporation stage, at least for peripheral collisions with projectiles like Argon and lighter [2]. Indeed during the evaporation cascade, fragments suffer an appreciable mass loss and their neutron-to-proton ratio approaches values for which the probabilities to evaporate protons or neutrons are about equal; the fragments then populate the so-called "evaporation corridor" [3]. For heavy projectiles one may however hope that the degree of equilibrium of the neutron-to-proton ratio towards this evaporation corridor is large enough to provide an excitation energy measurement and allows to conclude if peripheral collisions are dissipative or not at relativistic incident energies.

1. Projectile-like fragment yields

A $52 \mu\text{m}$ ^{197}Au target was irradiated with a 200 MeV/u ^{84}Kr beam at Saturne facility for this purpose [4], [5]. The projectile-like fragments, PLF, were detected with the SPES4 magnetic spectrometer equipped with an ionisation chamber and parallel plate avalanche counters. Contour plots of the N - Z distributions are given by thin dashed lines in Fig. 1.

In order to make quantitative comparisons we performed a simulation based on the geometrical prescription of the participant-spectator model [6], [7]. For primary isotopic distributions, gaussian shape is assumed which width is supposed to result from zero-point motion of the giant dipole resonance of the projectile [8]. The excitation energy, calculated from the surface energy excess prescription, is of about 2 MeV per abraded nucleon. The secondary N - Z distribution is deduced from the primary one by applying the evaporation code LOTO [4].

† *deceased*

This calculation is a Monte-Carlo method which uses the same transmission coefficients as those from LILITA code. It only takes into account proton, neutron, gamma and alpha particle emission ; it is assumed that the influence of fission is negligible. The most probable N/Z distributions predicted by this calculation lead to the thick line in Fig. 1. It clearly shows that the participant-spectator model underestimates the energy deposited in prefragments. The experimental ridge is well reproduced only if the excitation energy is multiplied by a factor 10 at least. This model assumes an unjustified sudden abrasion process. A more recent model from Gaimard and Schmidt described as the statistical abrasion model [9] takes the same geometry as the participant-spectator one and uses the hypergeometrical prescription to calculate the primary isotopic distribution. But the involved excitation energy comes from the mean energy induced by holes in the potential well below the Fermi surface, giving the missing factor of 10 mentioned above.

We compared these experimental fragment yields with an intranuclear cascade model too. The primary fragment distribution and involved excitation energies (predicted between 35 and 40 MeV per abraded nucleon) were calculated with the code ISABEL of Yariv and Fraenkel [10] and the evaporation code LOTO was applied to get the final fragment distribution. As shown by the thin ridge line in Fig. 1, this model fits the isotopic distribution centroids very well.

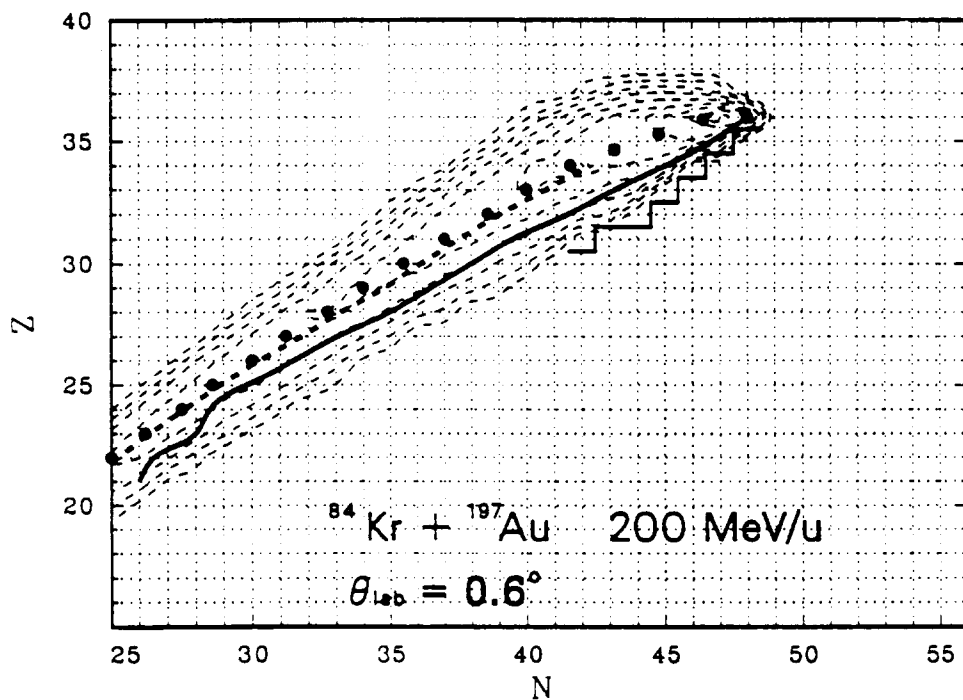


Figure 1: Isotopic distributions in the (N, Z) plane. Thin lines are iso-cross-section contours ; moving from one line to the next one, the cross-section scales by a factor 2. The broken line indicates the experimental cut due to the limited set of magnetic field values. The dotted line follows the ridge line of the isotopic distributions. The thick line is the ridge line predicted by the participant-spectator model. The dashed line results from the intranuclear cascade model [10].

These inclusive data suggest that the primary fragments undergo substantial excitation. This method used to determine the excitation energy remains however qualitative because residual fragmentation products are the same whatever could have been the energy deposited in primary fragments when it becomes large enough. This explains why the INC description or the statistical abrasion model are both able to reproduce the experimental results although there is a factor of two in the prediction of the excitation energy deposited in the fragments. Further inclusive experiments turn now to the study of specific channels [11]; so, to get exclusive data may be another way to draw other fragmentation mechanism outlines. We report here on the result of light charged particle multiplicities in the fragmentation of a 200 MeV/u ^{84}Kr beam impinging on a ^{59}Co target [12].

2. Experimental set-up

The experimental set-up was the same as the previous one with regard to the PLF detection. Four 14 cm thick Cesium-Iodine crystals, 3.3 cm in diameter, were placed in the target chamber to detect light charged particles. They were set out of plane and located between 5 and 10 degrees in the reaction plane. One cm thick plastic scintillator set in front of each CsI crystal defined the solid angle ($\Delta\Omega = 11$ msr).

Protons with energy larger than 238 MeV and the most part of deutons are punched through CsI crystals. In the two-dimensional fast-slow contour plot extracted from the CsI signals these particles fall in the same region as particles which escape from crystals laterally. An analytical calculation shows that 18 % of 200 MeV protons are so deflected due to the Coulomb multiple scattering on crystal ions. This would be in favour of an increase of the detector section but on the other hand, the pile-up rate reaches already 30 % for particles emitted in coincidence with a Cobalt fragment. It seems then difficult to reconcile these two aspects in an ideal CsI detector geometry.

We finally selected three classes of particles to construct multiplicity spectra: those with $Z = 1$, $Z = 2$ and the punched through particles. To take an event into account, both the CsI and the plastic signals had to give a consistent answer.

3. Experimental results

3.1. Neutron-rich nuclei production

Two situations could lead to neutron-rich nuclei. From a cold primary fragment, which leads to a short evaporation chain, the final nucleus will be able to get a large N/Z ratio. As prefragments are produced preferentially hot, this process is however quite improbable. On the other hand if a prefragment is normally excited, the only chance to get a neutron-rich nucleus is to select a very specific evaporation way. In this case the prefragment deexcitation must indeed lead to evaporation of a large number of protons as compared to neutrons.

These two possible mechanisms are finally expected to be equivalent as regards to their probability but we can hope to select one of them by looking at proton multiplicities, as shown in Fig. 2. If one assumes no fluctuation in the primary distribution (the excitation energy value per abraded nucleon remains constant and the N/Z ratio is chosen equal to the projectile value one), the yield of protons evaporated from the projectile increases with the PLF mass for nuclei with the highest N/Z ratios (dashed line). Then neutron-rich nuclei co-

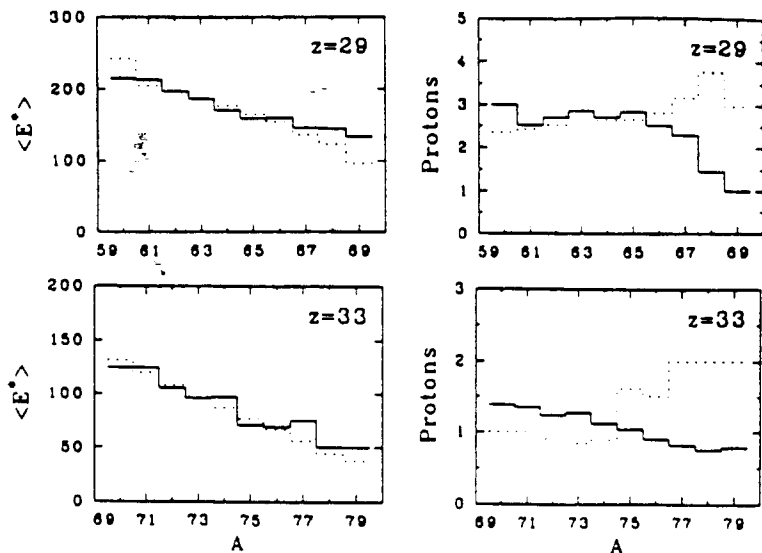


Figure 2: Mean excitation energy (left column) and mean value of the number of protons evaporated from the projectile (right column) for $Z=29$ and $Z=33$ PLF. The dashed line results from the simulation with no primary fluctuations, the thick line from the statistical abrasion model [9].

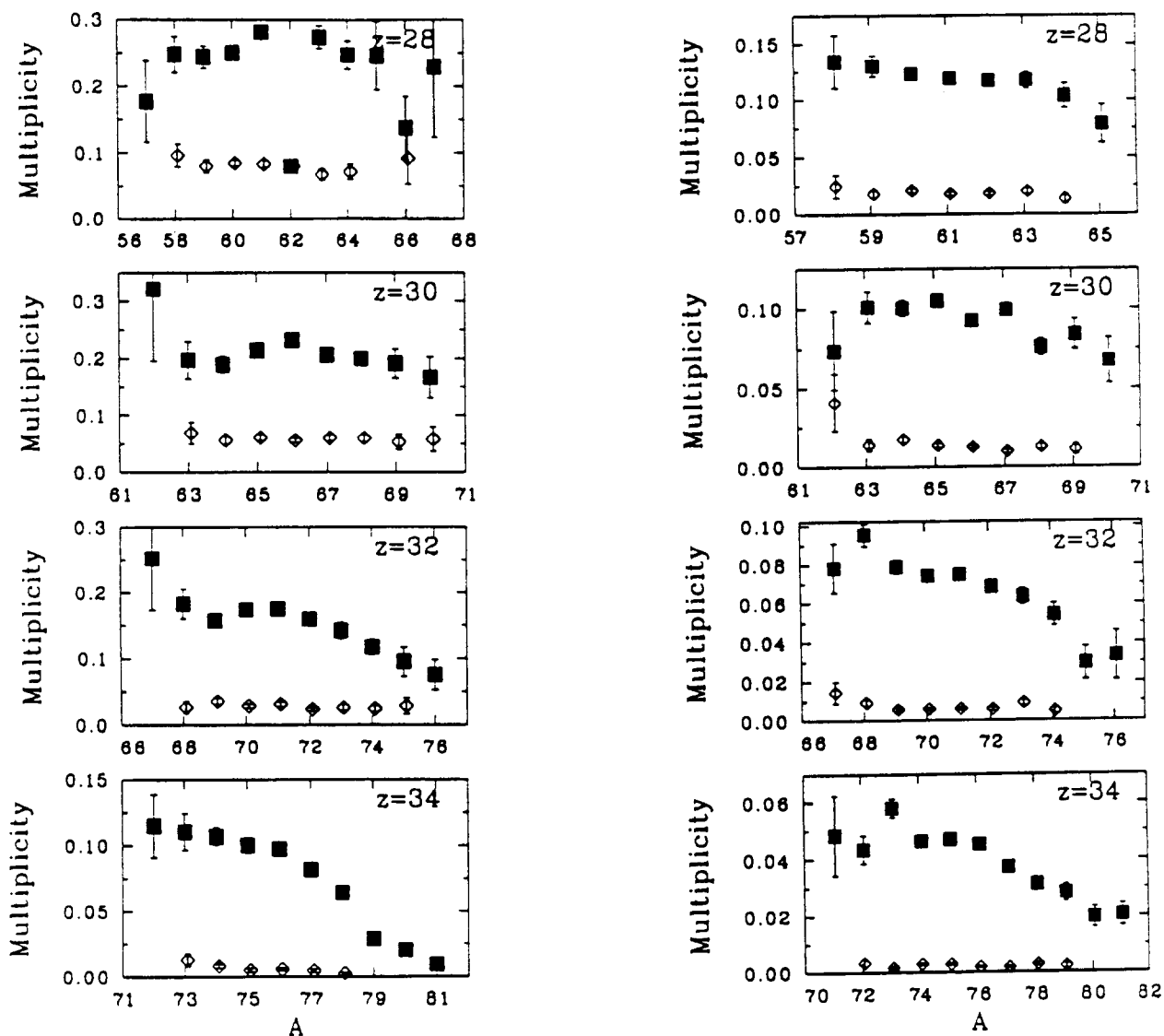


Figure 3: Multiplicity spectra for some PLF elements. Squares represent $Z=1$, diamonds $Z=2$ particle multiplicities. The left column refers to experimental data, the right one to intranuclear cascade model [10].

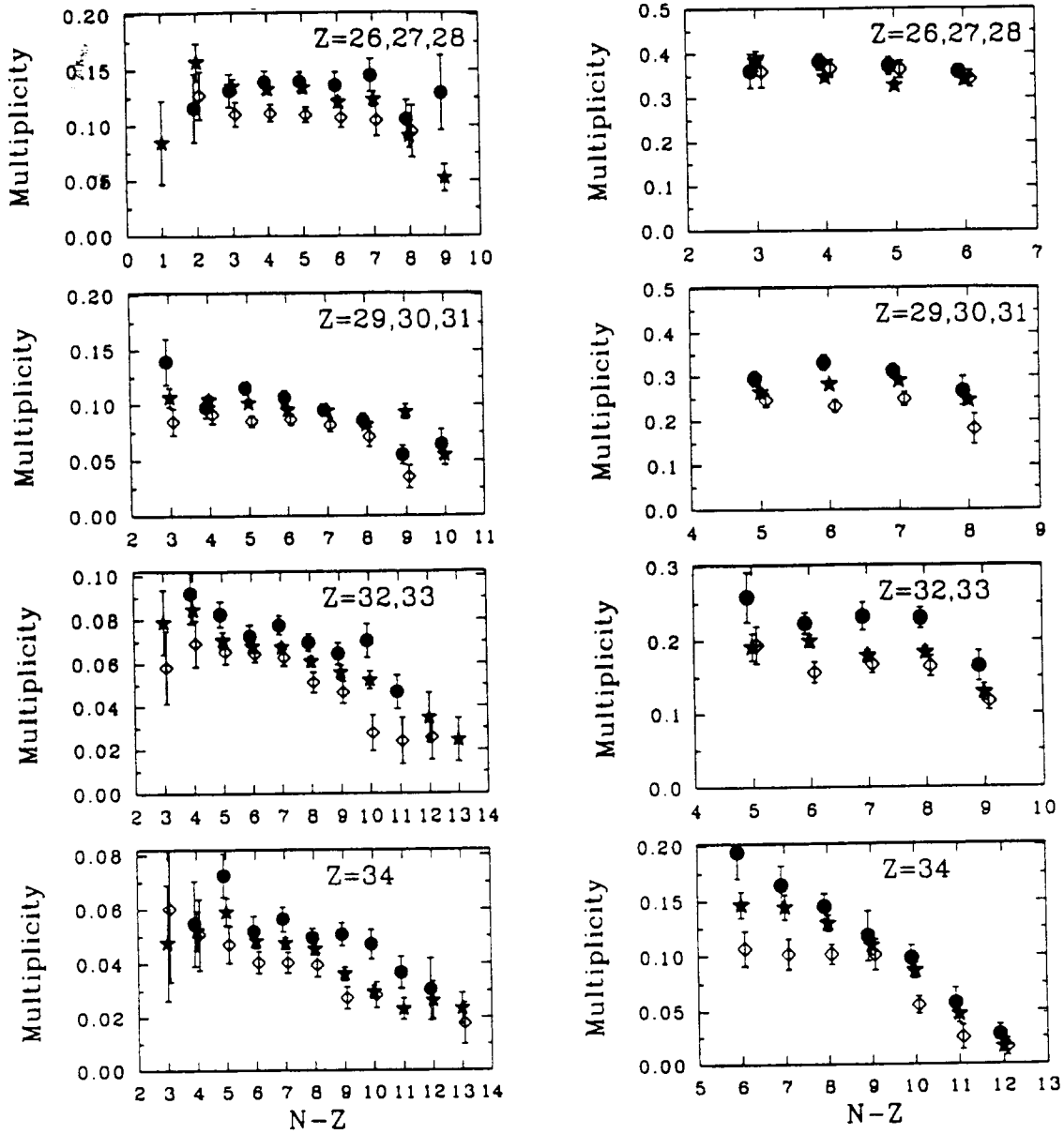


Figure 4: $Z=1$ particle multiplicity spectra associated with different fragment velocities for some PLF elements. Closed circles represent the low PLF velocity domain, stars the intermediate one and open diamonds the high one. The left column refers to experimental data, the right one to intranuclear cascade model [9].

me from fluctuations in the evaporation stage only, simulated by the code LOTO. Let us use the statistical abrasion model [9] described above, but with a mean excitation energy equal to 25 MeV per abraded nucleon as proposed by [11], to simulate primary isospin and excitation energy fluctuations ; the deexcitation is also calculated by the evaporation code LOTO. The neutron-rich nuclei are now linked with the lowest yield of protons evaporated from the projectile.

Multiplicities for $Z=1$ and $Z=2$ particles versus PLF masses are plotted in Fig. 3 for some elements. They clearly show that nuclei with large N/Z ratio are associated with low proton multiplicities. If most of

the detected particles are evaporation products, these data exhibit that these nuclei come from weakly excited prefragments.

As the pile-up is not taken into account in the intranuclear cascade simulation [10], as we don't accurately know the CSI crystal positions, experimental and simulated absolute values can't be strictly compared (a shift of 2 degrees towards large angles decreases the multiplicity by 30%). However the multiplicity evolution between different isotopes makes sense. It's noticeable that the intranuclear cascade model we used followed by the evaporation code LOTO, provides a multiplicity behaviour similar to the experimental one (see Fig. 3). In spite of the large average excitation energy predicted by this calculation, it is able to produce final fragments with a N/Z ratio larger than the projectile one, due to the large isospin and excitation energy fluctuations it predicts.

3.2. Excitation energy and fragment momentum correlations

If the large part of the detected particles comes from the evaporation stage, an observed correlation between the proton multiplicities and the PLF velocity may precise the reaction mechanism involved. For this purpose we divided the fragment velocity spectra in three parts and plotted the corresponding multiplicities in Fig. 4.

Particles emitted in coincidence with low velocity fragments provide the highest proton multiplicities ; one then observes a clear correlation between the excitation energy and the fragment momentum if the condition indicated above is well fulfilled. This correlation is nicely predicted by the intranuclear cascade model (see Fig. 4). On the contrary it can't be reproduced by the Goldhaber model [13]. This model assumes indeed that the reaction is dominated by recoil kinematic effects ; from this prescription the observed momentum width would result only from the nucleon Fermi distribution before the collision.

3.3. Nature of detected particles

Let us now show that the detected particles are mostly evaporation products. First of all the intranuclear cascade model predicts that the preequilibrium emission is insignificant between 5 and 10 degrees were the detectors are located (see Fig. 5). Furthermore the proton multiplicities behaviour for particles with energy larger and lower than 238 MeV gives an additional indication, Fig. 6.

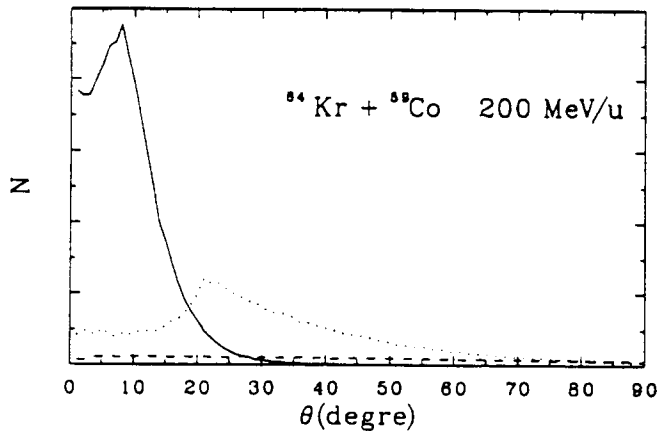


Figure 5: Angular distributions in the laboratory frame simulated by the intranuclear cascade model [10] for protons evaporated from the projectile (full line), from the target (dashed line) and for proton preequilibrium emission (dotted line).

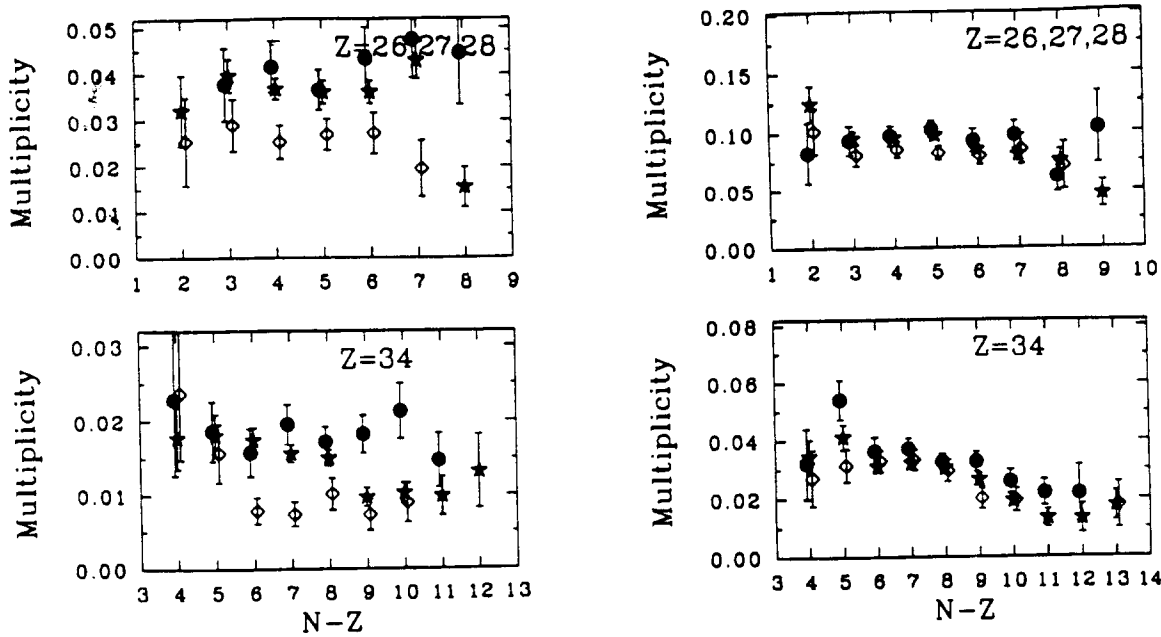


Figure 6: Experimental $Z=1$ particle multiplicity spectra associated with different fragment velocities. Closed circles represent the low PLF velocity domain, stars the intermediate one and open diamonds the high one. The left column refers to punched through particles (that is especially protons with energy larger than 238 MeV), the right one to $Z=1$ particles which stop in the CsI crystals (mostly protons with energy lower than 238 MeV).

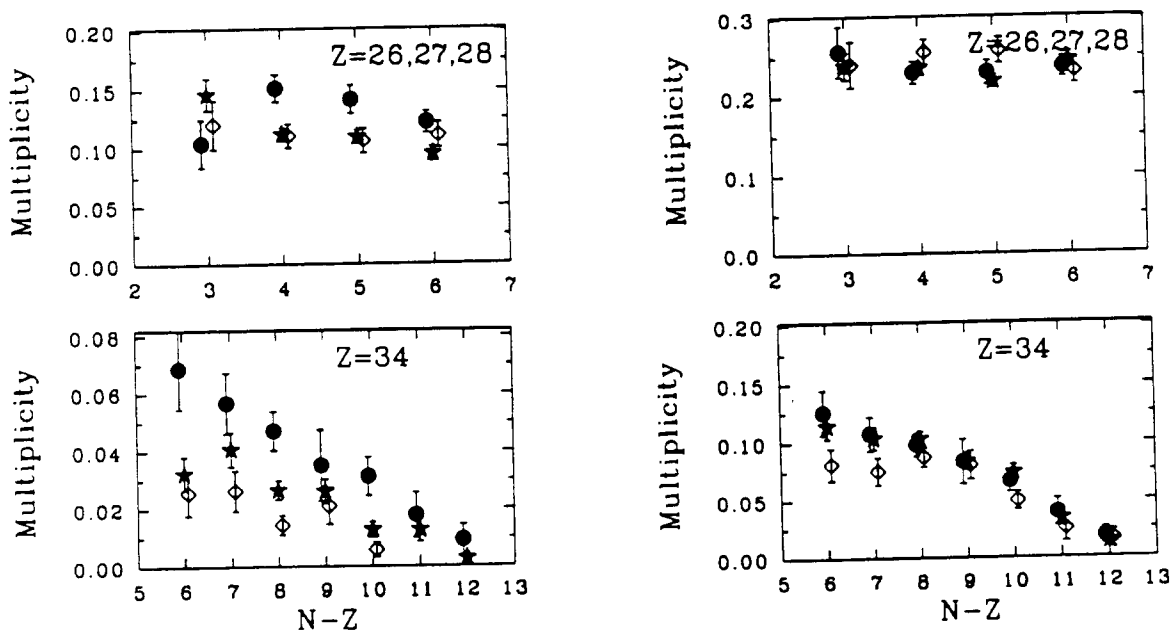


Figure 7: Proton multiplicity spectra associated with different fragment velocities simulated by the intranuclear cascade model [10]. Closed circles represent the low PLF velocity domain, stars the intermediate one and open diamonds the high one. The left column refers to protons with energy larger than 238 MeV, the right one protons with energy lower than 238 MeV.

Particles emitted in coincidence with low velocity PLF are favoured by the dissipative process in these two cases. But evaporation kinematics selects low momentum fragments for emitted forwards particles, that is high energy particles. One can then observe a clear correlation when high energy protons are selected. In the second case, the proton energy domain is large enough to accept all PLF velocities and the previous correlation is wiped out. One can finally explain these different situations by evaporation kinematic considerations. Moreover the intranuclear cascade model provides the same behaviour when only particles emitted from the projectile are plotted in Fig 7.

4. Conclusion

Fragment yields extracted from the inclusive experiment show that peripheral collisions are largely dissipative at 200 MeV/u incident energy. This result agrees with experiments performed with higher incident energies and heavier projectiles at GSI facility [11]; it was found there that inclusive data are also well reproduced if an excitation energy between 20 and 30 MeV per abraded nucleon is considered.

These dissipative aspects can be studied with more details from proton multiplicities. A clear correlation between the excitation energy and the projectile-like fragment momentum proves indeed that the momentum width can't be fully explained only by a Goldhaber-like mechanism, that is by recoil kinematic effects. Furthermore one sees that neutron-rich nuclei come from weakly excited prefragments. Exotic nuclei production consequently demands large primary isospin and excitation energy fluctuations. It's finally interesting to underline that the intranuclear cascade model seems to be a reliable framework to describe peripheral collisions at relativistic energies.

Références:

- [1] Y.P. Viyogi *et al.*, Phys. Rev. Lett. **42** (1979) 33
- [2] D.J. Morrissey *et al.*, Phys. Rev. Lett. **43** (1979) 1139
- [3] J.P. Dufour *et al.*, Nucl. Phys. **A387** (1982) 157c
- [4] L. Tassan-Got *et al.*, in Proc. XXVIII Winter Meeting on Nuclear Physics (Bormio, January 1990), ed. Ric. Sci. ed Educazione Permanente, suppl. 78 (1990) p. 361
- [5] C. Stephan *et al.*, Phys. Lett. **B262** (1991) 6
- [6] G.D. Westfall *et al.*, Phys. Rev. Lett. **37** (1976) 1202
- [7] J. Gosset *et al.*, Phys. Rev. **C16** (1977) 629
- [8] D.J. Morrissey *et al.*, Phys. Rev. **C18** (1978) 1267
- [9] J.J. Gaimard, K.H. Schmidt, Nucl. Phys. **A531** (1991) 709
- [10] Y. Yariv, Z. Fraenkel, Phys. Rev. **C24** (1981) 488
- [11] K.H. Schmidt, Phys. Lett. **B360** (1993) 313
- [12] C. Donzaud, Ph. D thesis, Université Paris XI (1993)
- [13] A.S. Goldhaber, Phys. Lett. **B53** (1974) 306